Generating Synthetic Computed Tomography (CT) Images to Improve the Performance of Machine Learning Model for Pediatric Abdominal Anomaly Detection

Samayan Bhattacharya* Avigyan Bhattacharya* Sk Shahnawaz
Jadavpur University, India
{samayan.bhattacharya, avigyanbhattacharya123, skshahnawaz072}@gmail.com

Abstract

Abdominal pain is one of the most common symptoms for a wide range of conditions in children, under the age of 16 years. Due to the limited ability of X-ray to distinguish between structures in soft tissue, physicians often rely on Computed Tomography (CT) scan to diagnose the underlying cause of abdominal pain. A CT scan exposes the patient to 70-150 times the radiation used for an X-ray. Moreover, CT scanning equipment is often not available in low-resource countries, leading to improper diagnosis and treatment. Children are more susceptible to the harmful effects of radiation than adults and might have limited language skills, based on age, and hence limited ability to describe their symptoms to the physician. In this work, we show that it is possible to use a Machine Learning (ML) model, capable of generating synthetic CT scans, from orthogonal X-ray scans, to improve the automatic prediction of abdominal anomalies. In particular, we focus on the detection of structural anomalies such as malformed organs, cysts, and appendicitis. On average, we are able to improve the performance of the prediction model by 9.75%, with respect to the model trained on only X-ray and 4.55%, with respect to the model trained on only generated CT scan, by training it on both the generated CT scan and X-ray.

1. Introduction

Abdominal pain (APN) is a very common symptom among children, accounting for around 5-10% of children brought to the emergency department (ED) [8]. APN, originating from a non-traumatic cause and lasting more than 5 days is called acute APN. APN may have a wide variety of causes, ranging from self-limiting ones to life-threatening ones. The causes are also classified as urgent, requiring immediate medical attention, and non-urgent, which do not progress in severity very rapidly. An effective diagnosis of the underlying cause(s) of APN allows early and more accurate management and leads to more positive outcomes and lower morbidity.

Accurate diagnosis in the medical field is the process of identifying a medical problem by analyzing the patient's symptoms and the results of medical imaging tests. There are many different types of medical imaging technologies available, including ultrasound (US), X-rays, MRI, CT scans, and NMR. X-ray was discovered by Wilhelm Roentgen in 1895 and it allows us to non-invasively look inside the human body. While a single 2D X-ray image is able to accurately represent the structure of hard tissue, such as bones, cartilage, and teeth, it does not produce an easily discernible representation of soft tissue. To address this issue, Computed Tomography (CT) imaging was developed. CT scan uses a large number (at least 100) of 2D X-ray images to construct a 3D volume representing the structures inside the body. While this makes it easier to discern soft tissue structures, the dose of radiation, to which the patient is exposed is increased by a factor of 70 to 150. While this is harmful to any human being, children are especially susceptible to such a high dose of radiation [35].

As mentioned earlier, APN stems from a wide range of causes, that vary according to the age and sex of the patient. The lack of classical expression of specific symptoms in some instances makes it more difficult to accurately diagnose the cause. This leads to a higher need for imaging or exploratory surgical procedures [32, 6, 47].

Apart from the risks associated with such practices, CT scanning equipment is expensive and inaccessible to patients in resource-constrained areas [34, 36]. Due to a lack of infrastructure, such as sanitation, APN is quite common among children in such areas. Physicians who are unable to access a CT scan often have to rely on their best judgment and provide a diagnosis based on their past experience alone. Hence, pediatric patients, with relatively rare conditions, get misdiagnosed, leading to morbidity or mortality.

*Authors contributed equally

Even if they have access to CT scanning equipment, reports are often delayed due to repair, and lack of sufficient radiologists or radiology technicians.

Synthetic CT scans can not only improve access to radiology but also reduce radiation exposure. Recently, a variety of methods have been proposed to automatically identify anomalies in medical images using deep learning (DL) [27]. In this work, we use DL algorithms to generate CT scans from 2 orthogonal X-ray images [53]. X-ray images are produced by passing X-ray through the body of the patient, onto a 2D surface, producing a 2D image. In CT scan, a rotating X-ray tube is used to capture multiple 2D images which are combined by computer algorithms to produce a 3D representation of the internal structures of the body. Given, the low variability of the human body, a DL model, trained on sufficient data, can generate a CT scan from an X-ray image. Generative Adversarial Networks (GANs) have been proven to be very effective in generating synthetic data [16]. Such data can be used by physicians or automatic classification algorithms. In this study, we used a Machine Learning (ML) model to classify image data as normal or abnormal. We show that we are able to improve the performance of the classification model by 9.75%, with respect to the model trained on X-ray and 7.55%, with respect to the model trained on only generated CT scan, by training it on both the generated CT scan and X-ray. The patients whose images are classified as abnormal may then be asked to undergo further investigation in the form of a CT scan.

For generating the synthetic CT scans, we use an existing DL model called X2CT-GAN [53]. This model is trained to generate CT scans from posterior-anterior (PA) and optionally lateral X-ray(s). It was trained on X-rays generated from CT scan using digitally reconstructed radiographs (DRR) technology [33]. The model was further trained to accept real X-ray images using style transfer by CycleGAN [56]. Further information about the X2CT-GAN model can be found in [53]. We use this synthetic CT scan, along with the X-ray images to train an ML algorithm to classify them as normal or abnormal. Due to the lack of large-scale abdominal X-ray datasets, we also used DRR to generate X-ray images from abdomen-pelvis CT images and then refined the model by training it on a smaller dataset of real X-ray images. The contributions of this work are as follows:

- We show that synthetic CT scans can be used to significantly improve the performance of an algorithm for the automatic classification of abdominal imaging as normal or abnormal.
- We provide an extensive evaluation of the proposed approach with convincing quantitative and qualitative results.
- We create a small-scale dataset of pediatric abdominal X-ray images, labeled as normal or abnormal.

2. Related Work

2.1. ML for Disease Classification

Artificial intelligence (AI) for automated image-based disease detection and segmentation has gained significant traction over the last decade [7, 40, 45, 55] from traditional ML methods such as applying logistic regression to heart disease prediction to achieve early detection of heart disease [24] to DL models achieving high success in classifying diseases from medical images [4]. In the context of heart diseases, Ansari et al. [2], for example, offered an automated coronary heart disease diagnosis system based on neurofuzzy integrated systems where as with the advent of DL in the subsequent years, Miao et al. [31], offered a DL-based technique to diagnosing cardiotocographic fetal health based on a multiclass morphologic pattern. Along the similar lines of solving disease classification using AI, there have been a substantial number of research studies that have focused on other types of diseases, such as kidney disease [29, 1], breast cancer [3, 48], diabetes [52], and Parkinson's disease [51, 15]. In recent times, these models have been used to classify COVID-19 [17], and other infectious diseases from X-ray images [43]. CT images have also been used for disease classification [12], as they provide additional context [58]. In particular, neural networks have been shown to be effective in classifying structural anomalies from CT scans [5, 38]. Multi-modal models, which fuse information from multiple sources, have also been shown to be effective for disease classification [28]. For example, models that fuse CT and electronic health records have been shown to improve prediction accuracy [20]. Similarly, models that fuse different views of chest X-rays have also been shown to improve prediction accuracy [19, 57]. One such study [37] presents a model which uses an intermediate bidirectional fusion architecture to extract and fuse the spatial correlation between the frontal and lateral views of X-rays. The fusion of X-ray and CT has been shown to be particularly effective for automatically diagnosing infectious diseases, such as COVID-19 [30].

2.2. Synthetic Data Used in Medical Imaging

Generative models, such as GANs [14] have made it possible to create realistic synthetic medical data [9, 13, 18, 23, 22]. This data has been used to address limitations on real data availability, such as limited availability [11] or class imbalance [25]. For example, synthetic images have been shown to be effective in chest pathology classification [41] and the localization of important anatomical landmarks [49]. [26] generated synthetic glioblastoma multiforme (GBM) in 2D magnetic resonance images with a

segmentation mask while [46] used a conditional GAN to generate synthetic polyp data from real edge-filtered images and a randomly generated mask. Another study [50] introduces a synthetic data generation pipeline that can be used to produce alternative artificial segmentation datasets with corresponding ground truth masks. Synthetically generated CT images have been widely applied for multiple medical image analyses, such as super-resolution [54], classification [11], and segmentation [42]. In this work, we use a recent GAN-based approach [53] to generate CT images from X-rays to improve the detection of structural anomalies in abdominal imaging. To the best of our knowledge, we are the first to use synthetically-generated CT images for the analysis of structural anomalies in abdominal imaging.

3. Structural Anomalies in the Abdomen

Children are often born with congenital anomalies. In some instances, there is an absence of an expression till several years after birth. For example, atrial septal defect (ASD) is often first detected after the child starts having physically demanding activities. Some defects never have an expression during the life of the individual, such as renal agenesis i.e. being born with a single kidney. The other kidney is able to perform the necessary functions and the individual may never experience any difficulty.

Another congenital structural anomaly is inguinal hernia, which makes up about 80% of hernias in children. The protruding part of the intestine may enter the scrotum, in males or the labia, in females, causing pain [44]. Some other forms of pediatric hernia are Umbilical hernias, Epigastric hernias, Hiatal hernias, and Incisional hernias. Umbilical hernias occur in babies, younger than 6 months, when the opening where the umbilical cord exits the abdomen fails to close. Epigastric hernias occur, mostly in males, as a protrusion through the abdominal muscle, between the chest and belly button. Hiatal hernias occur when the upper part of the stomach protrudes through a weak part of the diaphragm, where the esophagus meets the stomach. Incisional hernias occur after surgery, when the intestine protrudes through the abdomen, close to the incision site.

Cysts can occur at various locations inside the abdomen. Some common ones include ovarian cysts, renal cysts, and adrenal cysts. These might express in the form of symptoms like difficulty breathing, APN due to intestinal blockage, jaundice, etc. Cysts may or may not grow with time and may or may not cause any major problems in the long run. It is important to detect and, if necessary, remove the cyst early, before it causes any major issue or becomes more difficult to remove surgically. While cysts are often hollow, filled with fluids, tumors are solid masses of cells. A tumor may be benign or malignant. A benign tumor stays where it is and may or may not grow in size. A malignant tumor has a high probability of metastasizing i.e. spreading to other organs. Hence management of malignant tumors is more time sensitive than that of benign tumors.

4. Proposed approach

We use a generative model, designed to synthesize CT scans using orthogonal X-ray images [53], to test if the images produced by it can improve the accuracy of an ML model in classifying abdominal X-ray images. For an image to be classified as abnormal, we considered some common structural anomalies, namely, malformed organs, hernias, cysts, and tumors.

Let, x_i be an image in the X-ray dataset, consisting of a posteroanterior (x_i^{PA}) and a lateral (x_i^L) view of the patient. Hence, x_i=$[x_i^{PA}, x_i^L]$. Let, c be the generative model to produce synthetic CT scans. For a given x_i, c_i is the CT scan produced. Hence, $c_i = c(x_i)$. Let, c_i contain N slices and let s_i be a subset of all the slices in c_i. We train an ML model f to classify whether an image is normal or abnormal, using 3 different subsets s_i. These are described as follows:

- 50 % of slices are randomly removed. $\rightarrow (s_i^1)$
- Only odd-numbered slices are considered. $\rightarrow (s_i^2)$
- We consider exponentially decreasing number of slices, moving from the slice at the center to either end. Hence, if there are N slices, $centre = N/2$ and if j_{th} slice is considered, the next slice to be considered is the $(j + \alpha e^{abs(j-centre)})_{th}$ slice. The value of α is determined such that the total number of slices considered $\approx N/2$. $\rightarrow (s_i^3)$

Let the predicted value be g_i such that $g_i = f(v_i)$, where $v_i \in \{(s_i, x_i), (s_i, x_i^{PA}), (s_i, x_i^L)\}$ and $s_i \in \{s_i^1, s_i^2, s_i^3\}$. Here, g_i is a binary variable such that a value of 1 indicates that the image is abnormal and a value of 0 indicates that it is normal. The ML model f used is described in the following sections.

5. Experimental setup

5.1. Dataset

Abdominal X-ray is seldom used for diagnosing the cause of non-traumatic APN. Therefore, to our knowledge, there are no large-scale pediatric abdominal X-ray datasets. For this study we use the CT scan dataset provided by [21].

The dataset consists of abdomen-pelvis and chest-abdomen-pelvis CT scans, collected from 359 pediatric subjects, with ages ranging from 5 days to 16 years. The average age of the subjects is 7$\pm$ 4.5 years and the median age is 6 years. The cohort included 179 female and 180 male patients. The data was collected from three scanners, namely Somatom DefinitionAS+(Siemens Healthineers AG, Erlangen, Germany), LightSpeed VCT (GEHealthcare, Chicago,

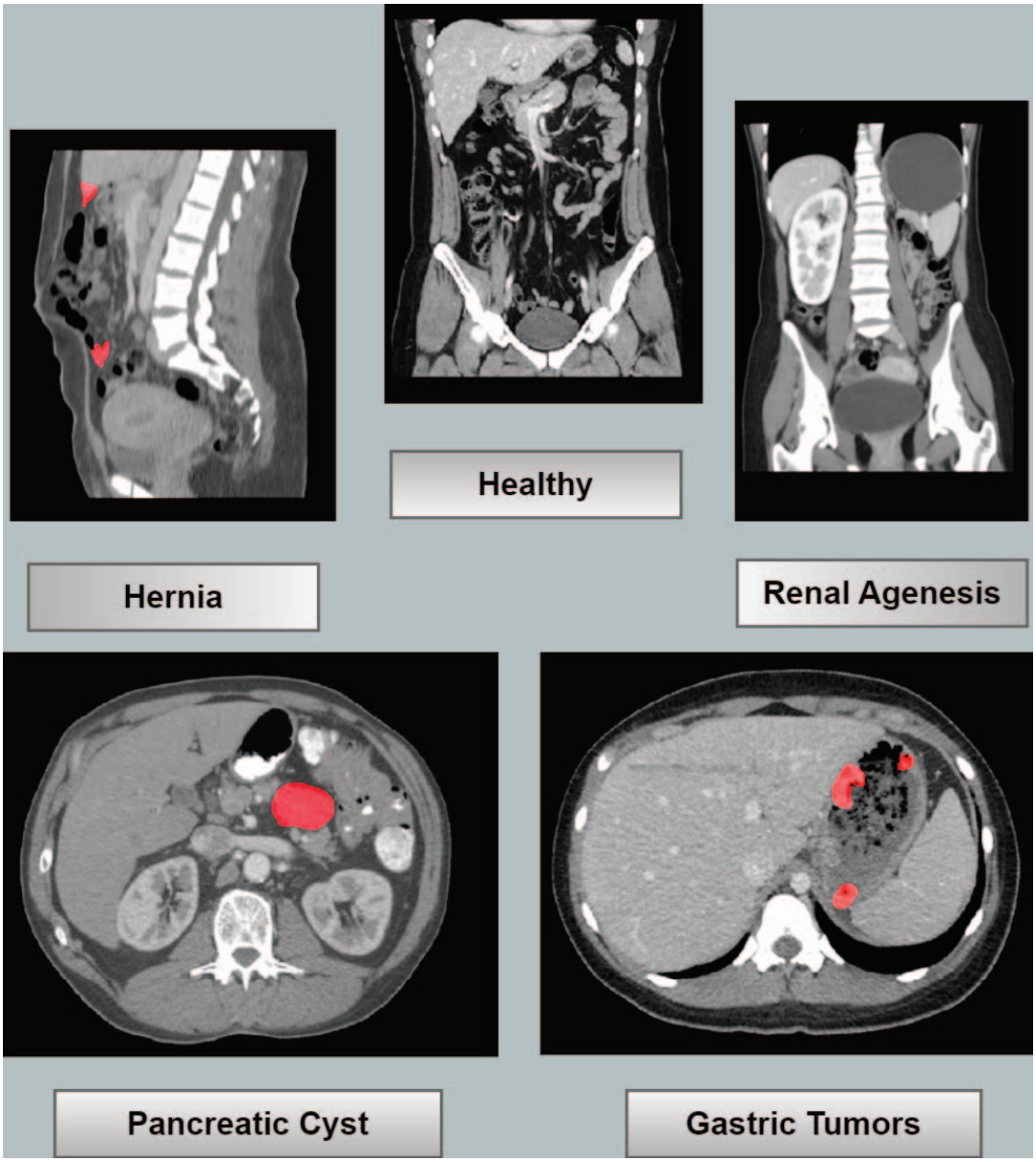

Figure 1. Examples of different types of structural anomalies considered in abdominal CT scans. These are, malformed organs, such as a missing kidney (renal agenesis), hernia, cysts, and tumors. The slice in which an anomaly is most distinct is shown, with the anomaly depicted in red, for representation purposes only. The slices used for training and testing are as described in Section 4
.

Illinois, USA), and Revolution (GE Healthcare, Chicago, Illinois, USA), at Children's Wisconsin. Twenty-five structures in the pelvis, abdomen, and thorax were retrospectively and manually contoured by four expert medical analysts. However, these scans didn't have any labels for anomalies. Hence, five radiologists, with over 10 years of experience, labeled each CT scan as "normal" or "abnormal", according to the criteria mentioned in the previous section. If any major structural anomaly, not included in these selection criteria, existed in an image, the radiologists were free to exercise their judgment to label that image as "abnormal" as well.

Digitally reconstructed radiographs (DRR) technology [33] was used to obtain the PA and L X-ray images from each CT scan. These were then used to generate synthetic CT scans using [53].

The dataset was divided into training and test sets in the ratio 9:1. For testing our approach, in addition to 10% of the data, mentioned above, we also used abdominal X-ray images collected at 10 rural medical centers located in dif-

ferent parts of the state of West Bengal in India. The size of the dataset was equivalent to 10% of the dataset provided by [21]. The ages of the subjects for this dataset ranged between 1 year and 14 years, with an average age of 10 years and a median age of 9 years. The cohort was 49% male and 51% female. The data was collected from random pediatric cases based on routine clinical indications, using a 3.5kW machine, operating at 55kVp. These X-ray images were labeled by the same 5 radiologists, who labeled the [21] dataset, according to the same criteria.

5.2. ML model architecture and training

5.2.1 Synthetic CT scan generation

We used a publicly available pre-trained version of X2CT-GAN [53] for generating CT scans using biplanar (PA and L) X-ray images. The model is trained on pediatric abdominal CT scans, provided by [21]. The training was performed in the same manner as in [53].

5.2.2 Image classification

For the classification of multimodal images (slices from the synthetic CT scan + biplanar X-ray images), we use the TransMed architecture, proposed by [10]. ResNet34 is used as a backbone for the CNN branch and DeiT-Small (DeiT-S) for the transformer branch. The generated CT scan, with 50% of the slices discarded, and the biplanar X-ray images were used. The images were first preprocessed using OTSU [39]. They were resized to 448x448. Data augmentation was performed using random flip, with a probability of 0.5, and Gaussian noise, with a mean of 0 and variance of 0.1.

We train the model with stochastic gradient descent (SGD) optimizer, with a momentum of 0.7, a learning rate of 10^{-3}, and a batch size equal to 2.

The model is tested on a dataset consisting of biplanar X-ray images, obtained using DRR, from 10% data of the [21] dataset and an equal number of real biplanar X-ray images. The real X-rays are transformed to match the style of the generated X-rays, using a CycleGAN [56].

6. Results

6.1. Quantitative analysis

We analyze the performance of the model, for classifying images as normal and abnormal, in terms of accuracy, sensitivity, and specificity. The results are shown in Table 1. We see that the model performs slightly better when X-ray images, along the PA plane, are provided along with the generated CT scans, than when X-ray images, along the L plane, are provided with the generated CT scans.

The best performance is obtained from using 50% of slices from the generated CT scan. As shown in Table 2, the results are better than using all the slices of the generated CT scan. The difference, in accuracies, between the two is 7%. This is probably because the slices towards the center of the generated CT scan are more distinct than those towards either end. This may be justified by the fact that the PA and L views, of the X-ray images, used to generate the CT scans, intersect at the center, providing much more information to the X2CT-GAN model about the structures at the center than those at positions away from the center. We also observe that using the slides from the original CT scan produces a difference in accuracy of 4% with respect to the accuracy when 50% of slides from the generated CT scan are used.

We test three approaches for selecting 50% of the slices in the generated CT scan. Using an exponentially decreasing number of slices, as we moved away from the center, produced the best performance. This might be explained by finding the projections of different slices on the two orthogonal planes (PA and L). The information density i.e. the

Data	Accuracy	Sensitivity	Specificity
$s_i^1 + x_i$	0.72	0.7	0.76
$s_i^2 + x_i$	0.79	0.74	**0.89**
$s_i^3 + x_i$	**0.83**	**0.81**	0.87
$s_i^3 + x_i^{PA}$	0.77	0.73	0.85
$s_i^3 + x_i^{L}$	0.76	0.73	0.82
$s_i^2 + x_i^{PA}$	0.74	0.69	0.84

Table 1. Evaluation of the performance of the model in classifying images as normal or abnormal, in terms of accuracy, sensitivity, and specificity. The variables, namely s_i^1, s_i^2, s_i^3, x_i, x_i^L, and x_i^{PA}, used to describe the different types of data used are explained in Section 4. The best results are shown in bold.

Data	Accuracy	Sensitivity	Specificity
All slices of synthetic CT scan + x_i	0.76	0.72	0.84
Original CT scan + x_i	**0.87**	**0.83**	**0.95**

Table 2. Evaluation of the classification performance of the model when all the slides of the synthetic CT scan and those of the original CT scan are used, along with the biplanar X-ray images.

Data	Accuracy	Sensitivity	Specificity
X-ray (biplanar)	0.73	0.67	0.85
Generated CT	0.79	0.75	0.87
Generated CT + X-ray	**0.83**	**0.81**	**0.87**

Table 3. Performance metrics for the model trained on biplanar X-ray images, 50% of the generated CT scan (s_i^3) and both.

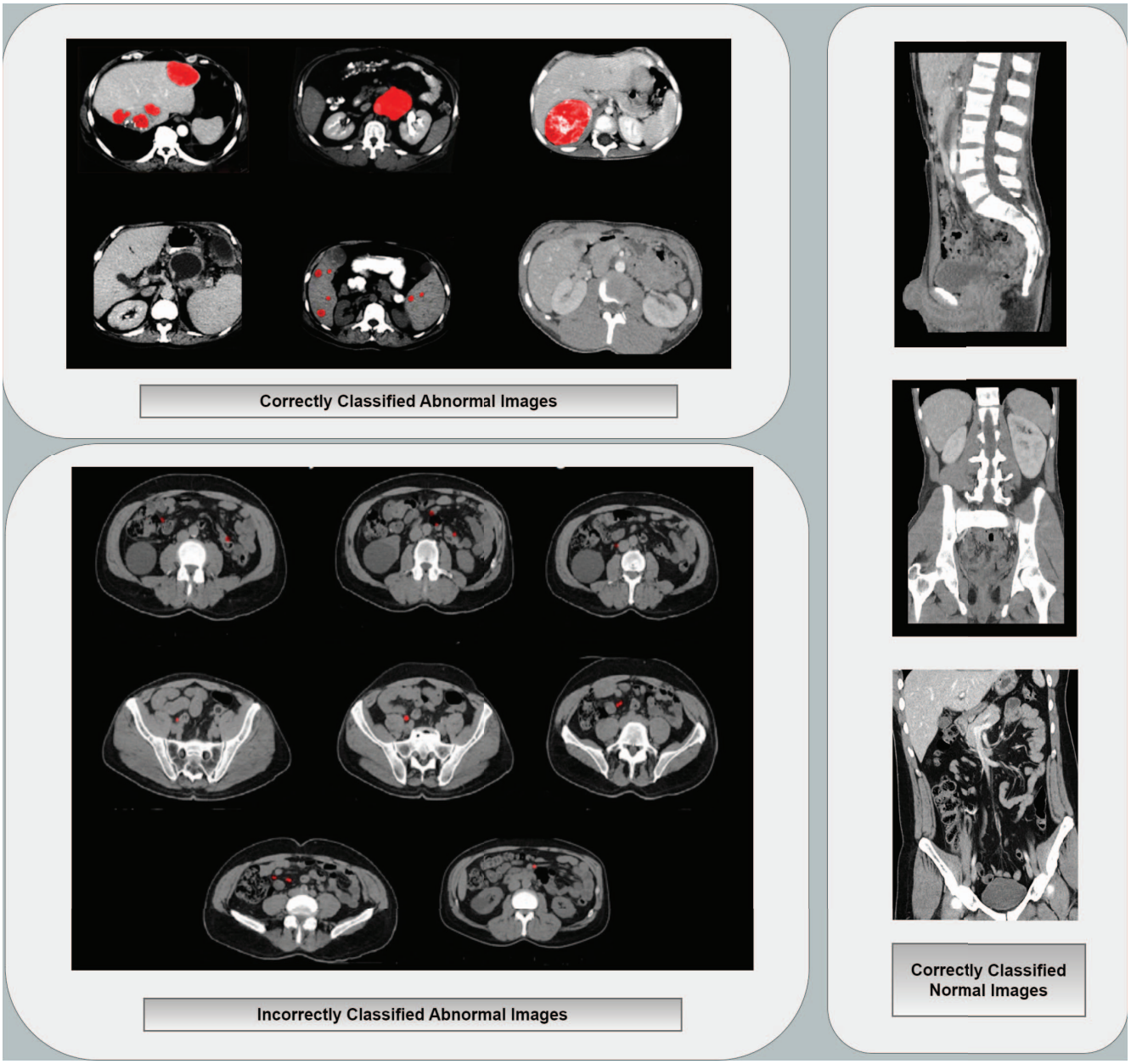

Figure 2. Examples of normal and abnormal CT scans most often correctly and incorrectly classified by the model.

amount of structural information obtained from the PA and L X-ray images, decreases according to a function that resembles the exponential function for a limited range of values, as we move away from the center. Hence, reducing the number of slices considered, accordingly, allows the model to focus on more reliable data, towards the center.

Another interesting observation is that the model has a higher specificity than sensitivity for all kinds of data used. This indicates that the model is able to classify healthy patients, or normal images, more reliably than abnormal images.

As shown in Table 3, the model performs better, when trained on both Generated CT scans and X-rays, as compared to when it is trained on either X-ray or the Generated CT scan.

6.2. Qualitative analysis

At last, we analyze the performance of the model qualitatively. As mentioned in the quantitative analysis, the model is able to classify normal images more reliably than abnor-

mal images. This is probably because the X2CT-GAN is able to generate normal structural features more accurately than abnormal ones. As shown in Figure 2, the images correctly classified most often are the normal images and the abnormal images with large, distinct anomalies. The images incorrectly classified most often are the ones with smaller, more distributed anomalies.

7. Conclusion and future work

In this paper, we proposed using generated CT scans to improve the detection of anomalies in pediatric abdominal imaging. Furthermore, the generated CT scans may be used by physicians to gain insight into the structural features in the abdominal cavity. This would not only be able to improve patient care in underserved areas, lacking access to CT scanning equipment but also reduce radiation exposure for pediatric patients by a factor of 70-150. It would also allow patients to avoid recurring costs and radiation exposure during follow-ups.

We have considered only a small subset of the possible structural anomalies that may cause non-traumatic APN in pediatric patients. We didn't consider any of the functional anomalies, such as infection, allergy, or a condition such as Crohn's disease. Hence, the proposed approach is far from a comprehensive diagnostic tool. The main purpose of our approach is to predict which patients need further investigation by means o an actual CT scan or investigative surgery, etc. To develop a comprehensive diagnostic tool, one might use other modalities of clinical data, such as blood, urine, and stool tests, in addition to imaging data.

In this work, we also labeled the images in the [21] dataset as normal or abnormal. These labels would be provided to any researcher, upon request. We also created a small-scale biplanar X-ray dataset, with the images labeled as normal or abnormal. This is made publicly available at `https://github.com/Skshanawaz072/Abdonimal-X-Ray-Dataset`.

References

[1] Ahmed J Aljaaf, Dhiya Al-Jumeily, Hussein M Haglan, Mohamed Alloghani, Thar Baker, Abir J Hussain, and Jamila Mustafina. Early prediction of chronic kidney disease using machine learning supported by predictive analytics. In *2018 IEEE congress on evolutionary computation (CEC)*, pages 1–9. IEEE, 2018.

[2] Abdul Quaiyum Ansari and Neeraj Kumar Gupta. Automated diagnosis of coronary heart disease using neuro-fuzzy integrated system. In *2011 World Congress on Information and Communication Technologies*, pages 1379–1384. IEEE, 2011.

[3] Hiba Asri, Hajar Mousannif, Hassan Al Moatassime, and Thomas Noel. Using machine learning algorithms for breast cancer risk prediction and diagnosis. *Procedia Computer Science*, 83:1064–1069, 2016.

[4] Mihalj Bakator and Dragica Radosav. Deep learning and medical diagnosis: A review of literature. *Multimodal Technologies and Interaction*, 2(3):47, 2018.

[5] Abhir Bhandary, G Ananth Prabhu, Venkatesan Rajinikanth, K Palani Thanaraj, Suresh Chandra Satapathy, David E Robbins, Charles Shasky, Yu-Dong Zhang, João Manuel RS Tavares, and N Sri Madhava Raja. Deep-learning framework to detect lung abnormality–a study with chest x-ray and lung ct scan images. *Pattern Recognition Letters*, 129:271–278, 2020.

[6] Priyadarshani R Bhosale, Marcia C Javitt, Mostafa Atri, Robert D Harris, Stella K Kang, Benjamin J Meyer, Pari V Pandharipande, Caroline Reinhold, Gloria M Salazar, Thomas D Shipp, et al. Acr appropriateness criteria® acute pelvic pain in the reproductive age group. *Ultrasound quarterly*, 32(2):108–115, 2016.

[7] James M Brown, J Peter Campbell, Andrew Beers, Ken Chang, Susan Ostmo, RV Paul Chan, Jennifer Dy, Deniz Erdogmus, Stratis Ioannidis, Jayashree Kalpathy-Cramer, et al. Automated diagnosis of plus disease in retinopathy of prematurity using deep convolutional neural networks. *JAMA ophthalmology*, 136(7):803–810, 2018.

[8] Kerry Caperell, Raymond Pitetti, and Keith P Cross. Race and acute abdominal pain in a pediatric emergency department. *Pediatrics*, 131(6):1098–1106, 2013.

[9] Edward Choi, Siddharth Biswal, Bradley Malin, Jon Duke, Walter F Stewart, and Jimeng Sun. Generating multi-label discrete patient records using generative adversarial networks. In *Machine learning for healthcare conference*, pages 286–305. PMLR, 2017.

[10] Yin Dai, Yifan Gao, and Fayu Liu. Transmed: Transformers advance multi-modal medical image classification. *Diagnostics*, 11(8):1384, 2021.

[11] Maayan Frid-Adar, Idit Diamant, Eyal Klang, Michal Amitai, Jacob Goldberger, and Hayit Greenspan. Gan-based synthetic medical image augmentation for increased cnn performance in liver lesion classification. *Neurocomputing*, 321:321–331, 2018.

[12] Min Fu, Shuang-Lian Yi, Yuanfeng Zeng, Feng Ye, Yuxuan Li, Xuan Dong, Yan-Dan Ren, Linkai Luo, Jin-Shui Pan, and Qi Zhang. Deep learning-based recognizing covid-19 and other common infectious diseases of the lung by chest ct scan images. *MedRxiv*, pages 2020–03, 2020.

[13] Amirata Ghorbani, Vivek Natarajan, David Coz, and Yuan Liu. Dermgan: Synthetic generation of clinical skin images with pathology. In *Machine learning for health workshop*, pages 155–170. PMLR, 2020.

[14] Ian Goodfellow, Jean Pouget-Abadie, Mehdi Mirza, Bing Xu, David Warde-Farley, Sherjil Ozair, Aaron Courville, and Yoshua Bengio. Generative adversarial nets. *Advances in neural information processing systems*, 27, 2014.

[15] Srishti Grover, Saloni Bhartia, Abhilasha Yadav, KR Seeja, et al. Predicting severity of parkinson's disease using deep learning. *Procedia computer science*, 132:1788–1794, 2018.

[16] Jie Gui, Zhenan Sun, Yonggang Wen, Dacheng Tao, and Jieping Ye. A review on generative adversarial networks: Algorithms, theory, and applications. *IEEE transactions on knowledge and data engineering*, 35(4):3313–3332, 2021.

[17] Hayden Gunraj, Linda Wang, and Alexander Wong. Covidnet-ct: A tailored deep convolutional neural network design for detection of covid-19 cases from chest ct images. *Frontiers in medicine*, 7:608525, 2020.

[18] Anant Gupta, Srivas Venkatesh, Sumit Chopra, and Christian Ledig. Generative image translation for data augmentation of bone lesion pathology. In *International Conference on Medical Imaging with Deep Learning*, pages 225–235. PMLR, 2019.

[19] Mohammad Hashir, Hadrien Bertrand, and Joseph Paul Cohen. Quantifying the value of lateral views in deep learning for chest x-rays. In *Medical Imaging with Deep Learning*, pages 288–303. PMLR, 2020.

[20] Shih-Cheng Huang, Anuj Pareek, Roham Zamanian, Imon Banerjee, and Matthew P Lungren. Multimodal fusion with deep neural networks for leveraging ct imaging and electronic health record: a case-study in pulmonary embolism detection. *Scientific reports*, 10(1):22147, 2020.

[21] Petr Jordan, Philip M Adamson, Vrunda Bhattbhatt, Surabhi Beriwal, Sangyu Shen, Oskar Radermecker, Supratik Bose, Linda S Strain, Michael Offe, David Fraley, et al. Pediatric chest-abdomen-pelvis and abdomen-pelvis ct images with expert organ contours. *Medical physics*, 49(5):3523–3528, 2022.

[22] Salome Kazeminia, Christoph Baur, Arjan Kuijper, Bram van Ginneken, Nassir Navab, Shadi Albarqouni, and Anirban Mukhopadhyay. Gans for medical image analysis. *Artificial Intelligence in Medicine*, 109:101938, 2020.

[23] Dimitrios Korkinof, Tobias Rijken, Michael O'Neill, Joseph Yearsley, Hugh Harvey, and Ben Glocker. High-resolution mammogram synthesis using progressive generative adversarial networks. *arXiv preprint arXiv:1807.03401*, 2018.

[24] Priyan Malarvizhi Kumar and Usha Devi Gandhi. A novel three-tier internet of things architecture with machine learning algorithm for early detection of heart diseases. *Computers & Electrical Engineering*, 65:222–235, 2018.

[25] Der-Chiang Li, Chiao-Wen Liu, and Susan C Hu. A learning method for the class imbalance problem with medical data sets. *Computers in biology and medicine*, 40(5):509–518, 2010.

[26] Lydia Lindner, Dominik Narnhofer, Maximilian Weber, Christina Gsaxner, Malgorzata Kolodziej, and Jan Egger. Using synthetic training data for deep learning-based gbm segmentation. In *2019 41st Annual International Conference of the IEEE Engineering in Medicine and Biology Society (EMBC)*, pages 6724–6729. IEEE, 2019.

[27] Geert Litjens, Thijs Kooi, Babak Ehteshami Bejnordi, Arnaud Arindra Adiyoso Setio, Francesco Ciompi, Mohsen Ghafoorian, Jeroen Awm Van Der Laak, Bram Van Ginneken, and Clara I Sánchez. A survey on deep learning in medical image analysis. *Medical image analysis*, 42:60–88, 2017.

[28] Manhua Liu, Danni Cheng, Kundong Wang, Yaping Wang, and Alzheimer's Disease Neuroimaging Initiative. Multi-modality cascaded convolutional neural networks for alzheimer's disease diagnosis. *Neuroinformatics*, 16:295–308, 2018.

[29] Fuzhe Ma, Tao Sun, Lingyun Liu, and Hongyu Jing. Detection and diagnosis of chronic kidney disease using deep learning-based heterogeneous modified artificial neural network. *Future Generation Computer Systems*, 111:17–26, 2020.

[30] Halgurd S Maghdid, Aras T Asaad, Kayhan Zrar Ghafoor, Ali Safaa Sadiq, Seyedali Mirjalili, and Muhammad Khurram Khan. Diagnosing covid-19 pneumonia from x-ray and ct images using deep learning and transfer learning algorithms. In *Multimodal image exploitation and learning 2021*, volume 11734, pages 99–110. SPIE, 2021.

[31] Julia H Miao and Kathleen H Miao. Cardiotocographic diagnosis of fetal health based on multiclass morphologic pattern predictions using deep learning classification. *International Journal of Advanced Computer Science and Applications*, 9(5), 2018.

[32] Diana L Miglioretti, Eric Johnson, Andrew Williams, Robert T Greenlee, Sheila Weinmann, Leif I Solberg, Heather Spencer Feigelson, Douglas Roblin, Michael J Flynn, Nicholas Vanneman, et al. The use of computed tomography in pediatrics and the associated radiation exposure and estimated cancer risk. *JAMA pediatrics*, 167(8):700–707, 2013.

[33] Natasa Milickovic, Dimos Baltas, S Giannouli, M Lahanas, and N Zamboglou. Ct imaging based digitally reconstructed radiographs and their application in brachytherapy. *Physics in Medicine & Biology*, 45(10):2787, 2000.

[34] Daniel Mollura and Matthew P Lungren. *Radiology in global health*, volume 1. Springer, 2014.

[35] Curtise KC Ng. Artificial intelligence for radiation dose optimization in pediatric radiology: A systematic review. *Children*, 9(7):1044, 2022.

[36] Patrick Sitati Ngoya, Wilbroad Edward Muhogora, and Richard Denys Pitcher. Defining the diagnostic divide: an analysis of registered radiological equipment resources in a low-income african country. *The Pan African Medical Journal*, 25, 2016.

[37] Jing Ni, Zubin Bhuyan, Qilei Chen, Xinzi Sun, Dechun Wang, Yu Cao, and Benyuan Liu. Enhance chest x-ray classification with multi-image fusion and pseudo-3d reconstruction. In *2022 International Joint Conference on Neural Networks (IJCNN)*, pages 1–8. IEEE, 2022.

[38] Masaki Ogawa, Masaya Kisohara, Tatsuhito Yamamoto, Shunsuke Shibata, Yoshinao Ojio, Kanako Mochizuki, Ayame Tatsuta, Shinichi Iwasaki, and Yuta Shibamoto. Utility of unsupervised deep learning using a 3d variational autoencoder in detecting inner ear abnormalities on ct images. *Computers in Biology and Medicine*, 147:105683, 2022.

[39] Nobuyuki Otsu. A threshold selection method from gray-level histograms. *IEEE transactions on systems, man, and cybernetics*, 9(1):62–66, 1979.

[40] Pranav Rajpurkar, Jeremy Irvin, Kaylie Zhu, Brandon Yang, Hershel Mehta, Tony Duan, Daisy Yi Ding, Aarti Bagul, Curtis P. Langlotz, Katie S. Shpanskaya, Matthew P. Lungren, and Andrew Y. Ng. Chexnet: Radiologist-level pneumonia detection on chest x-rays with deep learning. *CoRR*, abs/1711.05225, 2017.

[41] Hojjat Salehinejad, Shahrokh Valaee, Tim Dowdell, Errol Colak, and Joseph Barfett. Generalization of deep neural networks for chest pathology classification in x-rays using generative adversarial networks. In *2018 IEEE international conference on acoustics, speech and signal processing (ICASSP)*, pages 990–994. IEEE, 2018.

[42] Veit Sandfort, Ke Yan, Perry J Pickhardt, and Ronald M Summers. Data augmentation using generative adversarial networks (cyclegan) to improve generalizability in ct segmentation tasks. *Scientific reports*, 9(1):16884, 2019.

[43] Arun Sharma, Sheeba Rani, and Dinesh Gupta. Artificial intelligence-based classification of chest x-ray images into covid-19 and other infectious diseases. *International journal of biomedical imaging*, 2020:1–10, 2020.

[44] Sameh Shehata, Sherif Shehata, Herman L Wella, Mohamed Abouheba, and Ahmed Elrouby. Pediatric inguinal hernias, are they all the same? a proposed pediatric hernia classification and tailored treatment. *Hernia*, 22:941–946, 2018.

[45] Li Shen, Laurie R Margolies, Joseph H Rothstein, Eugene Fluder, Russell McBride, and Weiva Sieh. Deep learning to improve breast cancer detection on screening mammography. *Scientific reports*, 9(1):12495, 2019.

[46] Younghak Shin, Hemin Ali Qadir, and Ilangko Balasingham. Abnormal colon polyp image synthesis using conditional adversarial networks for improved detection performance. *IEEE Access*, 6:56007–56017, 2018.

[47] Martin P Smith, Douglas S Katz, Tasneem Lalani, Laura R Carucci, Brooks D Cash, David H Kim, Robert J Piorkowski, William C Small, Stephanie E Spottswood, Mark Tulchinsky, et al. Acr appropriateness criteria® right lower quadrant pain—suspected appendicitis. *Ultrasound quarterly*, 31(2):85–91, 2015.

[48] Zakia Sultana, MA Rahman Khan, and Nusrat Jahan. Early breast cancer detection utilizing artificial neural network. *WSEAS Transactions on Biology and Biomedicine*, 18:32–42, 2021.

[49] Brian Teixeira, Vivek Singh, Terrence Chen, Kai Ma, Birgi Tamersoy, Yifan Wu, Elena Balashova, and Dorin Comaniciu. Generating synthetic x-ray images of a person from the surface geometry. In *Proceedings of the IEEE conference on computer vision and pattern recognition*, pages 9059–9067, 2018.

[50] Vajira Thambawita, Pegah Salehi, Sajad Amouei Sheshkal, Steven A Hicks, Hugo L Hammer, Sravanthi Parasa, Thomas de Lange, Pål Halvorsen, and Michael A Riegler. Singan-seg: Synthetic training data generation for medical image segmentation. *PloS one*, 17(5):e0267976, 2022.

[51] Sarvesh Warjurkar and Sonali Ridhorkar. A study on brain tumor and parkinson's disease diagnosis and detection using deep learning. In *3rd International Conference on Integrated Intelligent Computing Communication & Security (ICIIC 2021)*, pages 356–364. Atlantis Press, 2021.

[52] Amani Yahyaoui, Akhtar Jamil, Jawad Rasheed, and Mirsat Yesiltepe. A decision support system for diabetes prediction using machine learning and deep learning techniques. In *2019 1st International informatics and software engineering conference (UBMYK)*, pages 1–4. IEEE, 2019.

[53] Xingde Ying, Heng Guo, Kai Ma, Jian Wu, Zhengxin Weng, and Yefeng Zheng. X2ct-gan: reconstructing ct from biplanar x-rays with generative adversarial networks. In *Proceedings of the IEEE/CVF conference on computer vision and pattern recognition*, pages 10619–10628, 2019.

[54] Chenyu You, Guang Li, Yi Zhang, Xiaoliu Zhang, Hongming Shan, Mengzhou Li, Shenghong Ju, Zhen Zhao, Zhuiyang Zhang, Wenxiang Cong, et al. Ct super-resolution gan constrained by the identical, residual, and cycle learning ensemble (gan-circle). *IEEE transactions on medical imaging*, 39(1):188–203, 2019.

[55] Zongwei Zhou, Md Mahfuzur Rahman Siddiquee, Nima Tajbakhsh, and Jianming Liang. Unet++: A nested u-net architecture for medical image segmentation. In *Deep Learning in Medical Image Analysis and Multimodal Learning for Clinical Decision Support: 4th International Workshop, DLMIA 2018, and 8th International Workshop, ML-CDS 2018, Held in Conjunction with MICCAI 2018, Granada, Spain, September 20, 2018, Proceedings 4*, pages 3–11. Springer, 2018.

[56] Jun-Yan Zhu, Taesung Park, Phillip Isola, and Alexei A Efros. Unpaired image-to-image translation using cycle-consistent adversarial networks. In *Proceedings of the IEEE international conference on computer vision*, pages 2223–2232, 2017.

[57] Xiongfeng Zhu and Qianjin Feng. Mvc-net: Multi-view chest radiograph classification network with deep fusion. In *2021 IEEE 18th International Symposium on Biomedical Imaging (ISBI)*, pages 554–558. IEEE, 2021.

[58] Liang Zou, Jiannan Zheng, Chunyan Miao, Martin J Mckeown, and Z Jane Wang. 3d cnn based automatic diagnosis of attention deficit hyperactivity disorder using functional and structural mri. *Ieee Access*, 5:23626–23636, 2017.